

ABLATIVE CARDIAC STEREOTACTIC BODY RADIATION THERAPY
STRUCTURE MAPPING

By

Ethan O. Cohen

A THESIS

Presented to the Medical Physics Graduate Program
and the Oregon Health & Science University
School of Medicine
in partial fulfillment of
the requirements for the degree of

Master of Science

June 2023

Table of Contents

Acknowledgements.....	ii
Abstract.....	iii
Introduction.....	1
Background.....	3
Ventricular Tachycardia and Potential Treatments.....	3
OHSU Ablative Cardiac SBRT Protocol and Workflow.....	5
Electro-Anatomical Mapping.....	7
XML File Format and Polygon Data.....	9
DICOM.....	11
Image Registration.....	12
Analyzing Image Registration Accuracy.....	12
Maximum Hausdorff Distance.....	12
Dice Coefficient.....	14
Methods and Materials.....	15
3D Slicer™.....	15
Varian Eclipse©.....	16
Python™ and PyCharm™.....	17
Mapping EAM to a DICOM Format.....	18
Determining Spatial Accuracy of EAM Displayed in 3D Slicer™.....	20
Comparing the XML EAM and DICOM EAM.....	22
Comparing Unhealthy Tissue shown in DICOM EAM to Treatment Target Volumes.....	23
Results.....	24
Results from EnSite™ and Slicer Distance Measurement.....	24
Results from XML EAM and DICOM EAM Segment Comparison.....	25
Results from Retrospective Analysis of Treatment Plans.....	26
Discussion.....	28
EnSite™ and 3D Slicer™ Distance Measurement.....	28
XML EAM and DICOM EAM Segment Comparison.....	28
Retrospective Analysis of Treatment Plans.....	29
Conclusion.....	31
References.....	33

Acknowledgements

I would like to show my most sincere gratitude to everyone at Oregon Health and Science University (OHSU) that was involved in the completion of this thesis project.

First, I would like to thank my thesis advisor Brandon Merz for providing invaluable support and guidance through this journey. The guidance, expertise, and feedback on my work has contributed greatly to the design and success of this project. The skills and knowledge provided was beneficial in achieving my academic goals and will continue to benefit me as I move forward towards my career as a medical physicist and for that I am grateful.

Secondly, I would like to show my gratitude to the other members of my thesis advisory committee Dr. Stephanie Junell, Dr. John Bayouth, and Dr. Saket Sanghai. The continued effort, enthusiasm, and insight has been instrumental in the completion of this project and helped make this a greatly enriching experience.

I would also like to show my thanks to all the medical physics staff, radiation oncology staff, and my fellow graduate students that I have had the pleasure to meet and become friends with over the course of my graduate studies. These connections have bolstered my passion for medical physics and made this journey an exceptionally pleasant experience.

Additionally, I want to thank my friends and family for the devoted encouragement, patience, and love during this challenging time. This support has kept me motivated during this journey and has led me to succeed in all my achievements over the course of this master's program.

Abstract

Purpose: To create a software tool that accurately reproduces eXtensible Markup Language (XML) format Electro-Anatomical Maps (EAMs) as a Digital Imaging and Communications in Medicine (DICOM) image. This will allow cardiac images to be imported into the Varian Eclipse© treatment planning system (TPS) for more accurate planning at Oregon Health and Science University (OHSU). The DICOM EAMs were also used to perform a retrospective analysis of past ablative cardiac Stereotactic Body Radiation Therapy (SBRT) treatments to assess plan quality. Ultimately the XML DICOM EAM mapping (XDEM) software tool will lead to better patient outcomes, more accurate treatment planning, and lower clinical cost.

Methods: XDEM was developed using Python™ and PyCharm™ and tested for spatial accuracy. XDEM's function was to map images in an XML format to a DICOM format. Two XML formatted EAM images were obtained prospectively and retrospectively for patients undergoing catheter ablation, which were then used for ablative cardiac SBRT treatment planning. Using distance measurements in EnSite Precision™ and 3D Slicer™ software, the percent differences were calculated to determine the fidelity of images displayed in 3D Slicer™. 3D Slicer™ was used due to its ability to import both DICOM images and XML EAMs. XDEM was then used to create a DICOM EAM, which was then imported into 3D Slicer™. The XML EAMs and DICOM EAMs were segmented and compared using the average hausdorff distance (AHD) and dice similarity coefficient (DSC). The DICOM EAMs with highlighted unhealthy tissue were then imported into Varian Eclipse© TPS and fused to the patients Computed Tomography (CT) image. The quality of the treatment plan was then assessed qualitatively.

Results: This study shows the results from three separate sub-projects related to validating 3D Slicer™, XDEM's mapping accuracy, and a retrospective analysis of past patient plans (n=2). Distance measurements were made between structures in 3D Slicer™ and EnSite Precision™ were shown to not be significantly different using a two tailed paired t-test. The segmented structures of the XML EAM and DICOM EAM were registered and analyzed, yielding a mean DSC of 0.979 and a mean AHD of 0.260 mm. The retrospective analysis showed that EAM structures could not be confidently aligned to the patient CT images, suggesting that further improvements must be made to register these images.

Conclusion: This study aimed to improve treatment planning accuracy, target validation, and clinical efficiency for ablative cardiac SBRT by creating a software tool that maps XML EAMs to DICOM EAMs. It was found that XDEM was able to map XML EAMs to DICOM with high fidelity. However, the retrospective analysis showed that it was difficult to confidently fuse DICOM EAMs to patient CTs, indicating the need for further research. This study provides insight into the accuracy and limitations of fusing EAMs to patient CTs for ablative cardiac SBRT and suggests further improvements to ultimately lead to better patient outcomes and lower clinical cost.

Introduction

Ventricular tachycardia (VT) treatments can vary widely depending on the extent of the damage to the cardiac tissue. For example, in some cases the first treatment will be to prescribe anti-arrhythmic drugs that return the patient's heart rate to a normal rhythm. If this approach is unsuccessful, the next step may be to ablate the unhealthy tissue with a specialized catheter that can deliver radiofrequency or cryo energy to the tissue. Finally, if neither of the previous treatments are successful, the physician may elect to treat the patient using ablative cardiac Stereotactic Body Radiation Therapy (SBRT).

Ablative cardiac SBRT was first used in the early 2010s to non-invasively ablate the unhealthy tissue of a patient experiencing VT with promising results¹. Since this first treatment, this procedure has gained credibility as a way to effectively treat patients with VT who have not responded to other, more common treatments².

During the treatment planning stage of this intervention at OHSU several cardiologists, radiation oncologists, physicists, and dosimetrists will be involved in determining what tissue is to be ablated and where to draw the radiation therapy target volumes. For this stage, data obtained during the unsuccessful catheter ablation procedure is brought over, such as a cardiac Electro-Anatomical Map (EAM), which shows the voltage potential of the cardiac substrate and in some cases, electrical activation during VT. Portions of the heart with low voltage (suggesting scar) as well as areas housing VT circuits are targeted for ablation.

The current standard of practice at OHSU is to perform cognitive fusion between the EAM and the patients Computed Tomography (CT) image. So, these images will be displayed on

separate monitors and as the cardiologist draws the target volumes on the patient's CT, they will reference the unfused EAM.

The aim of this research is to create the XML DICOM EAM mapping (XDEM) software tool that maps the eXtensible Markup Language (XML) formatted EAM into a Digital Imaging and Communications in Medicine (DICOM) format so that it can be imported into the treatment planning system used at OHSU, so that these images can be fused to one another. This will make it possible to see unhealthy cardiac tissue overlaid directly on top of the patient's anatomical CT image, which will potentially reduce error, allow for target verification, and save time and cost during this process.

Background

Ventricular Tachycardia and Potential Treatments

VT is a form of cardiac arrhythmia characterized by a rapid heart rate of over 100 beats per minute originating from the ventricles. This is a potentially life-threatening condition that can lead to sudden cardiac arrest or death in affected patients, and is responsible for approximately 300,000 deaths in the United States annually³. VT commonly arises from and is associated with other cardiac diseases such as coronary artery disease, myocardial infarction, or cardiomyopathy.

There are two main classifications for this condition, and whichever one the patient exhibits will determine whether the treatment is required. Sustained VT is defined as VT that lasts for more than 30 seconds, and requires some form of medical intervention, while VT that lasts less than 30 seconds is known as non-sustained VT, which may require medical intervention⁴.

There are a multitude of treatment types that can be conducted, and which one is decided upon depends on several factors, such as the arrhythmias severity, other underlying cardiac conditions, and which symptoms are present⁵. In some cases, the first step in treatment will be to use medications, such as a drug within an anti-arrhythmia class of drugs⁶. These drugs work by acting on cardiac ion channels to suppress or modify impulses that are either irregular or of an incorrect speed. These drugs are typically taken orally and over an extended period and can also be associated with significant adverse side effects and are not always effective depending on the extent of the cardiac disease.

For patients at elevated risk for VT recurrence with or without medications, implantable devices such as implanted cardioverter-defibrillators (ICDs) can be used to treat VT⁷. These

devices can detect cardiac arrhythmias and terminate them by delivering an electrical pulse to the cardiac tissue, which effectively resets the cardiac rhythm to normalcy.

Patients who have are unresponsive to the above treatments and are still experiencing recurrent VT may elect to receive an ablative procedure to cure their VT. There are two main categories of cardiac ablation, which include catheter ablation and ablative cardiac SBRT.

Catheter ablation can be an effective treatment and is usually the first choice of treatment for VT. This procedure involves locating a specialized catheter to the unhealthy cardiac tissue responsible for the arrhythmia so that it can deliver radiofrequency (RF) or cryo-energy and ablate the tissue⁸. This is a great treatment for patients that have normally structured hearts and whose tissue that is responsible for the VT is localized.

Ablative cardiac SBRT uses high energy x-rays to deliver energy to the cardiac tissue that is responsible for the patient's VT. Ablative cardiac SBRT is also non-invasive, making it the treatment of choice for patients unable to receive catheter ablation, or whose catheter ablation has failed in the past. A common reason for why patients would not be able to receive catheter ablation would be if their VT substrates are diffuse or inaccessible. During an ablative cardiac SBRT procedure, a single 25 Gray dose will be delivered to the cardiac tissue identified to be unhealthy in multiple coplanar arcs⁹.

Ablative cardiac SBRT is a potential option for treating VT in patients whose previous treatments have been unsuccessful or are not candidates for being treated through more typical therapies¹⁰. Using ablative cardiac SBRT to treat VT is also considered a new therapeutic option and a lot of research still needs to be done so that its effects and the safety behind this treatment are fully understood and only five patients have been treated at OHSU at the time this report was

written. However, even though this is a recently developed treatment type, patients treated have shown promising results¹¹.

OHSU Ablative Cardiac SBRT Protocol and Workflow

In this section, the protocol for interventional ablative cardiac SBRT at OHSU will be thoroughly explained.

At OHSU, there are several responsibilities that must be divided among radiation medicine staff when performing an ablative cardiac SBRT intervention. These responsibilities are related to patient simulation, treatment prescription, plan documentation, treatment planning and Quality Assurance (QA), and treatment setup, verification, and delivery.

The first step in these treatments is simulation. The purpose of this step is to simulate how the patient will be set-up during their radiation treatment, as well as obtain an anatomical CT scan that can be used for treatment planning and dose calculation. For this step, it is important that the physician, physicist, and radiation therapists are present to ensure accuracy. During the simulation, the patient will be placed head-first-supine in an immobilization device so that the setup is reproducible, and the patient's movement is minimal. The specific immobilization devices that are used are a wing board and thorax vacuum bag. It is important that the vacuum bag cradles the torso and has a well-defined arm position. This allows for a comfortable, reproducible, and accurate patient setup that reduces patient motion throughout the treatment and keeps the arms outside of the treatment field. The patient's arms will be above their head, and they will be holding onto the bars of the wing board. Each patient will have two CT scans unless otherwise noted by the physician; this will include both a free breathing CT with contrast and O-MAR (a metal artifact reduction algorithm) and a four-dimensional computed

tomography (4DCT). The free breathing CT will scan from the upper lungs to the bottom of the lungs, at least 5 cm above and below the heart. A 1 mm slice thickness will be used, the scan will take place 30 seconds after the contrast is administered, and the cardiac contrast protocol on the CT scanner will be used. For the 4DCT, the same bounds and slice thickness as the free breathing CT will be used, and this 4DCT will be taken after all contrast washes out of the patient's system; about 6 minutes. Other imaging that can be used for treatment planning may include a magnetic resonance imaging (MRI), positron emission tomography/computed tomography (PET/CT), and/or an EAM, which will be explained in the next section. Once all images are obtained and fused, the physicist and physician will review the accuracy.

Next is the prescription and treatment planning process. The organs at risk and the dose specifications that are considered during this procedure are the spinal cord, esophagus, stomach, lungs, and liver¹². Additional structures that are segmented include the right and left ventricles, as well as wires and any implanted devices that could be useful for image guided radiation therapy. The ITV is drawn on the untagged CT image that was obtained from the 4DCT, and the PTV is a 3 mm expansion of the of the ITV. Currently, when the ITV is being drawn by the physician, they will reference the EAM on a secondary monitor to define unhealthy tissue. This is the step that this project aims to streamline and make more accurate and efficient. The treatment type that is used is Volumetric Modulated Arc Therapy (VMAT) using a 6FFF photon beam with multiple coplanar arcs (3-4). Non-coplanar arcs may be used if required but are not typical. This procedure delivers 25 Gy to the PTV in one fraction unless otherwise specified by the physician.

Next, a series of quality assurance protocols must be performed to ensure that the treatment goes smoothly, and the patient receives the dose calculated by the TPS within an

allowable tolerance¹³. Radiation therapists are required to perform Image Guided Radiation Therapy (IGRT) QA to verify the accuracy of the imaging isocenter, radiation isocenter, image registration software, and couch isocenter. This is performed daily and overseen by the physicist. Additional QA may be performed by the physicist at their discretion. Patient specific QA is also required in preparation for this procedure. The gamma analysis criterion that is used is 3%/2 mm and requires a pass rate of greater than 90%¹⁴.

The final step in this process is treatment setup, verification, and delivery. The patient will be set up on the medical linear accelerator (LINAC) system's couch in the same way as they were during the simulation stage. This ensures that the patient's physical dose will be equal to the dose calculated by the TPS, within acceptable tolerances. During the treatment, it is required that the attending radiation oncologist, electrocardiologist, medical physicist, and radiation therapists are present. IGRT is also mandatory during this treatment since such a high dose is delivered per fraction, which must include volumetric imaging such as four-dimensional cone beam computed tomography (4DCBCT). Intrafraction imaging is also used to ensure the patient has not shifted out of tolerance intrafraction.

[Electro-Anatomical Mapping](#)

Electro-Anatomical (EA) mapping is a technique that is used in cardiac electrophysiology to create a 3D reconstructed image of cardiac tissue that shows both its anatomical structure and electrical behavior. EA mapping involves the use of a specialized catheter containing multiple electrodes and several electrodes that are placed on the surface of the patient. These electrodes are used to record electrical signals from the cardiac tissue, and then reconstruct the EAM of the

heart, which is finally used to determine what cardiac tissue is responsible for creating abnormal electrical signals and VT.

There are many EA mapping systems available but the one used at Oregon Health and Science University (OHSU) where this research was conducted is the Abbott EnSite Precision™ system¹⁵. This system includes a low powered magnet that is placed underneath the patient bed, a system reference surface electrode, six surface electrodes, and a diagnostic catheter electrode.

The low powered magnet placed underneath the patient creates a magnetic field that interacts with the catheter magnetic sensor. This sensor can detect changes in the magnetic field, which allows for precise catheter localization in real time.

The surface electrodes are placed anterior, posterior, left to right lateral, and superior (neck) to inferior (leg). These electrodes form three orthogonal axes with the heart at the center. An 8 kHz signal is then sent alternately through the pairs of surface electrodes. This signal can be sensed by the catheter electrode to determine the position of the catheter and allow the generation of 3D EAMs of cardiac anatomy. Then this system was tested for tracking accuracy, the mean accuracy error was 0.44 ± 0.45 mm (n=4032)¹⁶. This error is well below the PTV margin of 3 mm that is drawn during treatment planning for ablative cardiac SBRT.

EA mapping has transformed the field of electro-cardiology by allowing for the creation of 3D images with detailed anatomical and physiological information about the electrical activity of cardiac tissue (Figure 1).

The ability to localize abnormal cardiac tissue has greatly improved the success rate of ablative procedures and has made it possible to treat previously untreatable cardiac conditions. As EA mapping advances, so will the effectiveness and accuracy of these lifesaving procedures.

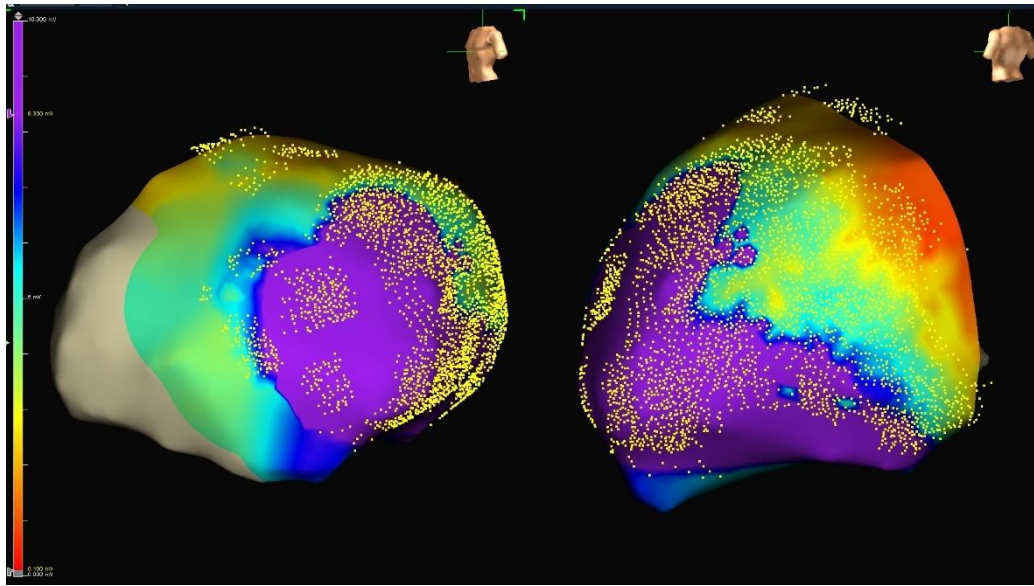


Figure 1: Example cardiac electro-anatomical map showing the electrophysiological information of the heart

XML File Format and Polygon Data

The data that is exported from the EnSite™ EA mapping software is in the XML format, which is a widely used file format for the exchange of data¹⁷. This is a particularly useful file format for storing structure data such as the polygon data that makes up cardiac EAMs.

The polygon data that is stored is used to represent many 2D shapes with a set of vertices, edges, and a scalar value designated to each vertex. Each vertex is represented by a point in three-dimensional space (x,y,z) and each edge is represented by a set of two vertices. In the case of these EAMs, the scalar value that is assigned to each vertex is the voltage potential at that anatomical location, which is determined during the EA mapping procedure. The polygons that are exported from EnSite™ are triangles, so each polygon will be represented by a 3-tuple where each index represents a vertex. So, if there is a list of vertices $(1,0,0)$, $(0,1,0)$, $(0,0,1)$, and $(1,1,1)$

and a polygon is represented as (2,4,1), the polygon's vertices will be located at (0,1,0), (1,1,1), and (1,0,0).

XML files that contain polygon data are typically formatted in a way that uses a specific arrangement of data. This arrangement defines the structure of the data, the name of each data value, the data type, and how each element relates to other elements. A simplified example of this data format can be seen below in figure 2.

```
<Vertices>
    40.2358  -108.1819  43.8933
    40.8806  -107.2758  43.7880
    39.9219  -107.2144  43.6586
    .
    .
<Vertices>
<Map_data>
    5.00000000
    5.00000000
    5.00000000
    .
    .
<Map_data>
<Polygons>
    2 1 3
    4 16 2
    1 6 5
    .
    .
<Polygons>
```

Figure 2: Format of data contained within XML file

For the storage of polygon data, a common schema that is used is the Geography Markup Language (GML)¹⁸. GML defines sets of elements that are used to represent geographic features such as polygons, as well as providing a standard format for how these features are encoded so that GML formatted XML files can be widely accepted into various software without issue.

DICOM

The Digital Imaging and Communications in Medicine (DICOM) standard was developed in the 1980s by the American College of Radiology (ACR) and the National Electrical Manufacturers Association (NEMA). The purpose of this standard was to help with the exchange of medical images between different medical imaging systems and devices. DICOM is used widely in the medical field, especially in medical subfields that extensively use medical imaging, such as cardiology, radiology, and radiation oncology so that images can be accurately stored, transmitted, and displayed¹⁹.

DICOM uses a hierarchical structure to organize medical image information. This information can include but is not limited to patient demographic information, parameters used during scan acquisition, image metadata, as well as the pixel data for the image itself. The DICOM standard also defines several elements that describe the context of the image such as what imaging modality, the body part that was imaged, and the orientation of the image.

There are many advantages to using the DICOM standard for medical imaging when compared to other image formats. DICOM images are completely self-contained which means that they contain all necessary information to interpret and display the image. This makes DICOM images completely independent of any device or software that is used to acquire, process, send, or view them. All of this is to ensure that regardless of what device is used to access the image, it will be viewed accurately and consistently by the clinician.

The DICOM standard is the foundation for how images are viewed, sent, and processed in medicine. Since it was initially developed, it has revolutionized the exchange of medical images which has greatly improved clinical efficiency, accuracy, and patient care.

Image Registration

Image registration is used widely in radiation oncology practice. It is used to accurately fuse medical images of different modalities. In radiation oncology, a Computed Tomography (CT) image may be registered to a PET image so that metabolic activity can be highlighted on the patient's anatomy²⁰. This can also be used during IGRT to match the patient's simulation CT to a Cone Beam Computed Tomography (CBCT) generated by the LINAC system²¹.

The process for image registration can be done multiple ways, such as rigid, affine, or deformable. It involves the identification of multiple similar anatomical landmarks in each image so that the images can be matched. These images can be shifted manually or by using a mathematical algorithm. Image registration is a critical step in radiation oncology that can determine the effectiveness of the patient's treatment²². In the context of this project, the patient's CT and EAM are fused so that the voltage map of the heart highlighting unhealthy tissue can be seen on the patient's anatomical CT image.

Analyzing Image Registration Accuracy

The metrics that were used throughout this project to determine the similarity between the XML EAM and the DICOM EAM were the maximum Hausdorff distance (MHD), average Hausdorff distance (AHD), and dice similarity coefficient (DSC). Each of these metrics will be thoroughly explained below.

Maximum Hausdorff Distance

The MHD, first introduced by Felix Hausdorff in 1914, is a measure of how similar or dissimilar two sets of points are in a metric space. This concept can easily be applied to the

comparison of two similar segmented objects that are contained within separate medical images. Below is a mathematical representation of how the MHD is calculated²³:

$$MHD(A, B) = \{\{d(a, b)\}\}$$

Where ‘a’ and ‘b’ are points within set ‘A’ and ‘B’ respectively, $h(a,b)$ is the MHD, and $d(a,b)$ is the Euclidean distance between points ‘a’ and ‘b.’ More simply, when the MHD is calculated, for each point in ‘A’ the distance the nearest point in ‘B’ will be determined. Then, the maximum distance from this set of distances will be the MHD.

The MHD allows the registration of two similar objects to be scored which can help determine whether the EAM has been properly mapped to the DICOM format. However, the MHD is not a perfect metric and can be sensitive to outliers.

A variant of the MHD that can be used for segment comparison is the AHD, which is mathematically defined below below²⁴.

$$AHD(A, B) = \frac{1}{N} \sum_{a \in A} \|a - b\|$$

The AHD is the distance from a point in one set to the nearest point in the other set (points being voxels in the context of this project), averaged across all points. There are several benefits to using the AVD when compared to the MHD. First, it is much less sensitive to outliers, because if there are several extreme values, their impact will be reduced when taking the average. This value also gives a much more intuitive understanding of the distance between each set since it represents the average distance between all points, rather than just a distance between two points. In the context of this project, both the MHD and AHD were calculated, however the AHD is much more indicative of XDEM’s ability to map XML EAMs to DICOM EAMs.

Dice Coefficient

The Dice similarity coefficient (DSC) is another measure that can be used to analyze how well two structures have been registered to one another. According to AAPM TG-132²², the DSC is defined as two times the volume of where the two segments overlap, divided by the total volume of the two segments combined. This gives a quantitative measure of how well the two segments are overlapping with each other. As the overlap approaches agreement, the DSC will go to one, and as the volumes diverge into nonoverlapping structures, the DSC will go to zero. So, the closer the DSC is to one, the more in agreement the two structures will be. The DCS can also be defined mathematically which is shown below²²:

$$\text{Dice coefficient} = 2 * |A \cap B| / (|A| + |B|)$$

It is shown in literature that segmentation DSC for head and neck treatments greater than 0.9 are acceptable for stereotactic radiosurgery applications²⁵.

Methods and Materials

This chapter will cover the various programs that were used throughout this project, as well as the methods for determining image mapping accuracy, and how previous treatments performed at OHSU were analyzed.

3D Slicer™

In this section a description of 3D Slicer™ and its features specific to this project will be explored. 3D Slicer™ is an open-source, extensible software platform designed for image visualization and analysis. This software has a large community of users with medical backgrounds such as medical imaging and surgical navigation, as well as other fields such as astronomy, paleontology, and 3D printing. This software allows users to interactively visualize, analyze, segment, and manipulate medical images. 3D Slicer™ has also shown acceptable accuracy as an image computing platform²⁶. In this section, the ways that this software was used in this project will be explained thoroughly.

The specific version of 3D Slicer™ that was used in this project was 3D Slicer™ 5.0.3. This older version (The cardiac-electrophysiology module for EAM import has not been updated for newer versions) is capable of importing 3D EAMs with the EnSite™ file export format. This allows for the direct comparison of the DICOM EAM to the original XML EAM that was obtained during the mapping process.

3D Slicer™ is used in this project as an image registration software and to perform a statistical analysis of how well images are registered using methods explained previously. 3D Slicer™ is capable of importing DICOM images as well as cardiac EAMs. Once both images are

imported, they can be segmented, manually registered, algorithmically registered, and then analyzed. This analysis is done using the MHD, AHD, and DSC.

Varian Eclipse©

This section will give a brief description and then explore the different features of the Varian Eclipse© TPS version 15.1 software in the context of this project.

Varian Eclipse© TPS is a comprehensive tool that is designed to generate highly accurate radiation therapy treatment plans. It offers many features that enable radiation oncologists, medical physicists, and dosimetrists to plan and optimize patient specific radiation therapy plans. The start-up window can be seen below in figure 3.

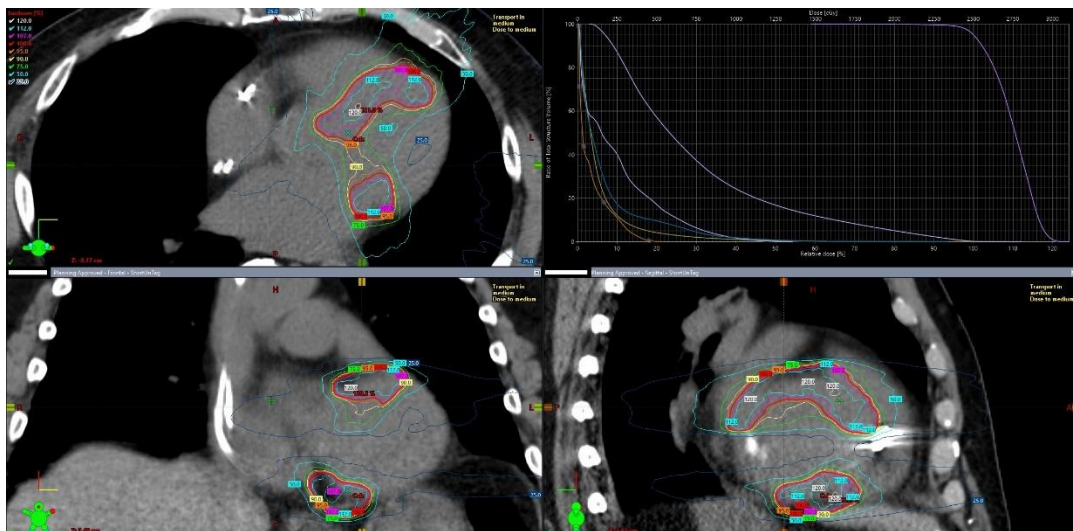


Figure 3: Example image of the Varian Eclipse© user interface

These features include external beam planning, contouring, image registration, administration, etc. However, the contouring and image registration were the only modules used during this project.

In the context of this project, Varian Eclipse© TPS was used to retrospectively analyze past patient treatment plans for ablative cardiac SBRT. The previously obtained EAMs were used to provide detailed information on the voltage potentials of the cardiac substrate. The fusion of the EAM and CT within Varian Eclipse© will allow the user to accurately identify unhealthy tissue on the CT image so that accurate target volumes can be delineated. The methods for this retrospective analysis are detailed later in this thesis.

Overall, Varian Eclipse© is a versatile and versatile radiation oncology TPS that gives the user access to advanced tools and algorithms to create and optimize patient specific treatment plans. It was essential to perform the retrospective analysis in this project due to its ability to fuse images and access past treatments performed at OHSU.

Python™ and PyCharm™

Python™ 3.9, the coding language used to create XDEM, is a powerful programming language for scientific applications. Python™ 3.9 was released on October 5, 2020, and is one of the most popular coding languages available²⁷.

Python™ has an easy to learn syntax, while remaining a powerful and capable tool that can be used for a wide variety of applications. These applications include web development, scientific computing, data analysis, artificial intelligence, and more²⁸.

Another main advantage of Python™ is that it is open source and has an active, large community that continues to develop Python's™ functionality and create new libraries that extend its capabilities.

Overall, Python™ is a versatile and powerful programming language that is used in a wide variety of fields. It is easy to learn and use, has a large community, and is very flexible making it popular for novice and experienced software developers alike.

PyCharm™ was also used over the course of this project to develop XDEM involved in converting XML EAMs to DICOM EAMs. PyCharm™ is a powerful integrated development environment (IDE) for the Python™ programming language. For this project specifically, PyCharm™ version 2022.3.2 was used and was downloaded from the JetBrains™ website²⁹.

PyCharm™ provides a user-friendly environment for software development and debugging Python code. Some helpful features of PyCharm™ include code highlighting, code analysis, debugging, and testing. PyCharm™ is also able to install and organize 3rd party plugins and libraries for ease of use.

PyCharm™ was an essential tool for developing XDEM. Its user-friendly interface enabled efficient and effective Python™ code development which led to the highly functional XDEM being produced.

Mapping EAM to a DICOM Format

The XDEM can convert an EAM that is in XML format into a DICOM image that can be imported into the Varian Eclipse© TPS. In this section, the process by which XDEM creates the DICOM map will be thoroughly explained.

First, several parameters must be set at the beginning of the code that heavily influence the final DICOM image. This includes the pixel dimensions, the slice separation, the voltage

threshold at which tissue is considered unhealthy, and patient information such as name and medical records number. In this section of the code, the path to the XML file that contains the EAM information that is exported from EnSite™ is also defined.

Next, XDEM accesses the data within the XML file and pulls out the locations of each vertex, the voltage values associated with each vertex, and the polygon data whose format is explained in earlier sections. These data are all stored in the form of a NumPy array while being processed by XDEM.

XDEM then determines the location of the cross-sectional planes, each of which will be a slice in the final DICOM image. It does this by finding the range in “Z” for all vertices and divides it by the set slice separation. This gives the number of slices and where they intersect the “Z” axis. Each slice will be parallel to the “XY” plane defined in the EnSite™ software. Once each slice is determined, XDEM will determine what polygons intersect each slice. For each polygon that is intersected, two points will be recorded which represent the intersection points. Finally, XDEM will draw a line between the intersection points in each polygon with the result being a cross section slice of the EAM.

Once the cross-section structures are determined, XDEM will begin to build the DICOM images. XDEM does this by binning the intersection lines into a pixel grid, the dimensions of which are set by the user. The dimensions that were used in this project were a 512x512 pixel grid, like a CT image, and a slice separation of 2 mm. These parameters allowed for good agreement between the XML EAM and the DICOM EAM, which will be seen in later sections. When building the DICOM images, XDEM also must override the DICOM tags from the sample CT image with the correct patient and the unique identifiers (UID), so that image can be

accepted into Varian Eclipse© and stored in the correct patient profile. A visual flowchart of this entire process can be seen below in figure 4.

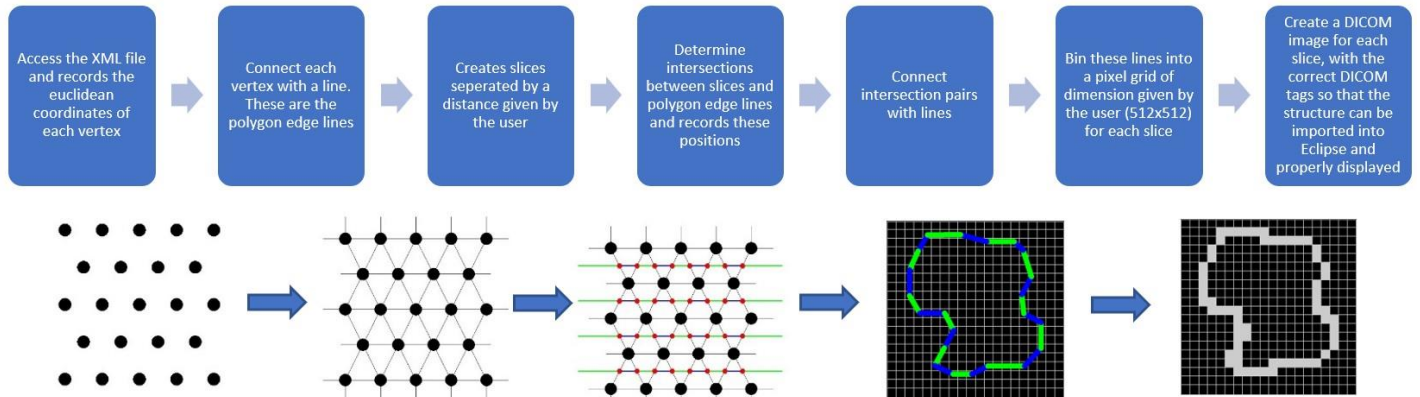


Figure 4: Visual representation of how the tool creates DICOM EAMs from XML EAMs

Determining Spatial Accuracy of EAM Displayed in 3D Slicer™

Before taking any measurements or performing data analysis within 3D Slicer™, it is important to determine how accurately the EAMs are being displayed. Otherwise, the accuracy of the EAM mapping to the DICOM format could not be determined with respect to the EAM within EnSite™.

The method for determining the accuracy of the EAM displayed in 3D Slicer™ involves the following steps. The EAMs that were used during this project were loaded onto the EnSite™ software and distance measurements between obvious structures were taken by a technician. The same EAMs were then imported into 3D Slicer™ and the same measurements were taken. The similarity of these measurements will show that the image is scaled properly when being displayed in 3D Slicer™.

For this project, an EnSite™ technician opened the EAMs of multiple patients that received ablative cardiac SBRT and took several reproducible distances measurements within the EnSite™ software. For each structure, the technician measured the anterior-posterior distance, the left-right lateral distance, and the superior-inferior distance. Some other measurements between obvious landmarks were also taken.

These structures were then accessed in 3D Slicer™ where the same measurements were taken. An example of a similar measurement being taken in EnSite™ and 3D Slicer™ can be seen in figure 5 below.

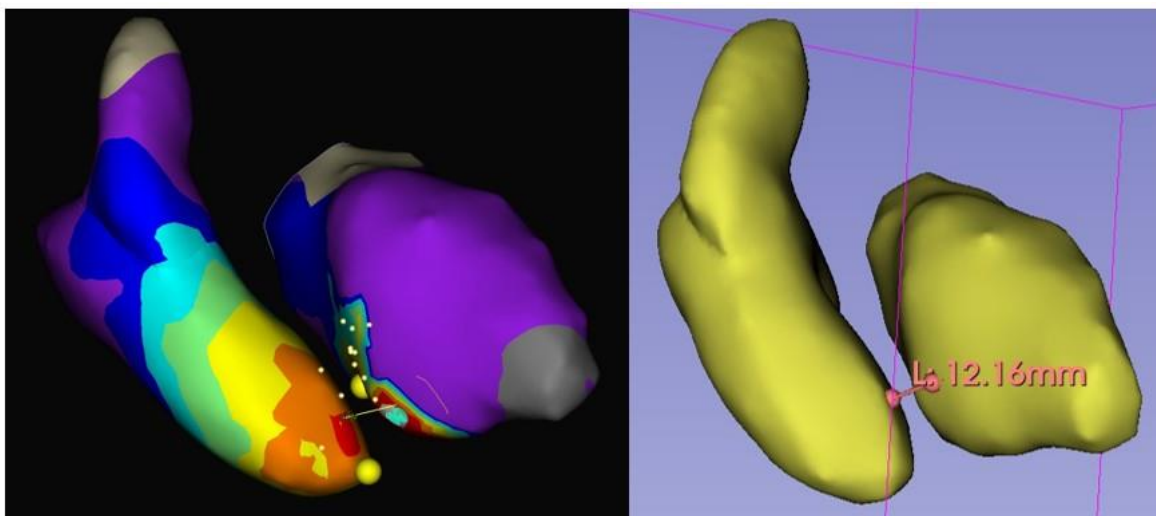


Figure 5: Similar distance taken in EnSite™ (Left) and 3D Slicer™ (Right). Both show roughly 12 mm.

Once the distances are measured and recorded, the differences in each measurement were calculated and a paired t-test was performed to determine if the measurements were significantly different from one another. For this two-tailed t-test, the significance level used was $\alpha = 0.05$.

Comparing the XML EAM and DICOM EAM

Since the EAM exported from EnSite™ and the DICOM EAM created in this project are in different formats, it was difficult to compare these images in their stand-alone form. It was determined that the best way to compare these images was to segment both surface structures, register them, and then calculate similarity coefficients outlined in TG-132²² as well as some other commonly used similarity coefficients. These similarity coefficients, which were explained in earlier sections are the DSC, AHD, and MHD.

First, both images were imported into 3D Slicer™ and segmented using the dedicated segmentation module. Next, the segments were registered using a manual registration. This was to get them close so that 3D Slicer's™ automatic iterative registration tool could maximize the segment overlap. Once these segments were registered to one another, the segment comparison module within 3D Slicer™ could be used to calculate the DSC, MHD, and AHD. Once this data was collected, it could be analyzed within Microsoft Excel to determine the validity of the structure mapping performed in this project. A flowchart of how this process was performed can be seen below in figure 6.

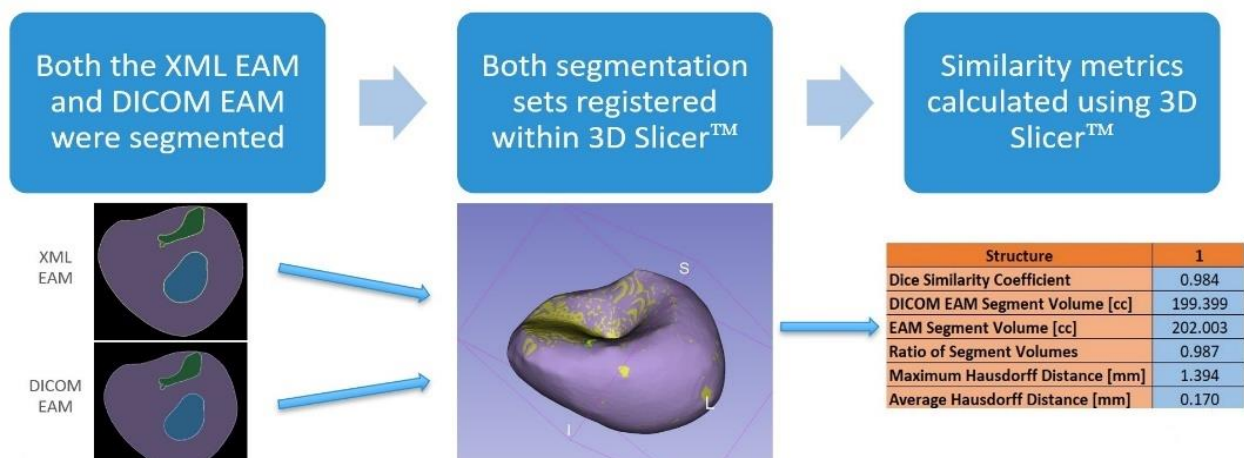


Figure 6: Flowchart for how the XML EAM and DICOM EAM were compared

Comparing Unhealthy Tissue shown in DICOM EAM to Treatment Target Volumes

For this subproject, a variant of XDEM was created for this project was created to highlight all tissue below a threshold voltage, which was set to 1.5 mV. An example image can be seen in figure 7. The unhealthy is displayed as a one-pixel expansion to the typical single pixel thick structure surface.

Once the DICOM EAMs with highlighted, this image can be imported into Varian Eclipse© TPS and fused to the patients CT image that was used for treatment planning for the actual procedure. All image registration within Varian Eclipse© was done manually due to the lack of obvious anatomical landmarks or fiducials that can be used for point-based image registration. Once the images were fused to the best of the user's ability, a qualitative assessment was performed just to see if the unhealthy tissue highlighted on the EAM lined up with the previously delineated PTVs. The reason a qualitative analysis was performed rather than a quantitative analysis, was because out of the four patients that have been treated at OHSU for VT, only two of them had their cardiac anatomy mapped using the EnSite Precision™ system. So, any values that were obtained would not give any statistical certainty.

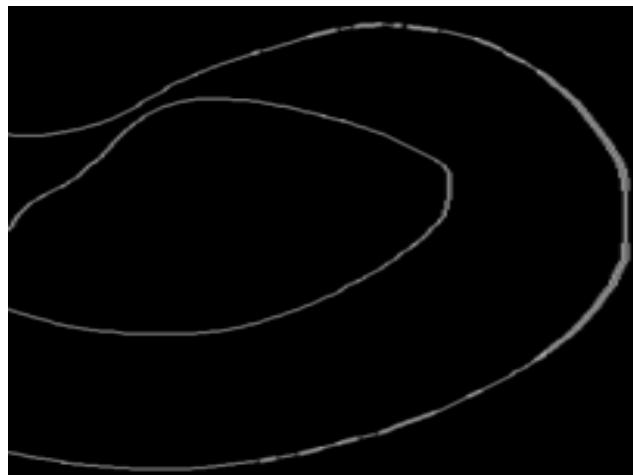


Figure 7: EAM with tissue below set threshold voltage highlighted. This can be seen on the right side of the image

Results

This chapter will explain the results that were received during the review of XDEM's ability to recreate EAMs in a DICOM format. This section will also detail the results from checking the fidelity of the images displayed in 3D Slicer™ when compared to EnSite™, and how well the target volumes were drawn in past ablative cardiac SBRT treatments at OHSU.

Results from EnSite™ and Slicer Distance Measurement

Distance measurements between obvious structures within several images were created on EnSite™ and copied within 3D Slicer™ and then recorded. For example, in figure 5 the distance between two key points can be seen first in the EnSite™ software and then in 3D Slicer™. This was then repeated for other structures from patients treated at OHSU with ablative cardiac SBRT.

Next, all distance measurements were compiled into a Microsoft Excel™ spreadsheet.

Table 1 shows the distances measured between key points in EnSite™ and 3D Slicer™, then shows the differences between these measurements, the mean of the differences, the standard

Table 1: Distance measurements between similar anatomical locations in EnSite™ and 3D Slicer™ as well as statistical analysis

Measurement	EnSite Precision™ [cm]	3D Slicer™ [cm]	Difference [cm]
1	12	12.16	-0.16
2	42	41.99	0.01
3	31	31.07	-0.07
4	89	88.89	0.11
5	50	50.05	-0.05
6	97	97.06	-0.06
7	42	42.02	-0.02
8	59	59.12	-0.12
9	37	36.96	0.04
10	40	40.03	-0.03
		Mean	-0.035
		STDV	0.073
		t score	-1.508
		p	0.166

deviation of the differences, and the values received from performing a two tailed t-test on these distances to determine whether the differences were statistically significant.

The mean difference between measurements made in EnSite™ and 3D Slicer™ was calculated to be -0.035 cm, the standard deviation was 0.0734 cm, and the p-score was determined to be 0.166 .

Results from XML EAM and DICOM EAM Segment Comparison

The EAM and DICOM EAM were both imported into 3D Slicer™, segmented, registered, and then analyzed using the process mentioned above. All data for this section was received from the dedicated radiation therapy segment analysis module within 3D Slicer™. This module provided the DSC, segment volumes, the HD, and AHD. This data as well as some other values that were automatically calculated by 3D Slicer™ can be seen below in Table 2.

Table 2: DSC, segment volumes, ratio of segment volumes, HD, and AHD of the

Structure	1	2	3	4	5	6	Mean
Dice Similarity Coefficient	0.990	0.984	0.960	0.984	0.971	0.987	0.979
DICOM EAM Segment Volume [cc]	1034.03	88.0374	26.6582	199.399	139.748	271.444	293.219
EAM Segment Volume [cc]	1018.87	85.7239	25.0309	202.003	146.274	278.114	292.669
Ratio of Segment Volumes	1.015	1.027	1.065	0.987	0.955	0.976	1.004
Maximum Hausdorff Distance [mm]	7.482	1.020	1.831	1.394	1.414	1.905	2.508
Average Hausdorff Distance [mm]	0.307	0.224	0.262	0.170	0.343	0.252	0.260

The mean DSC for all the structures analyzed was 0.979 , the ratio of segment volumes for each structure was 1.004 cc, the mean maximum MHD was 2.508 mm, and the mean AHD

was 0.260 mm for all structures. A visual representation of the DSC and AHD for each structure can be seen below in figure 8.

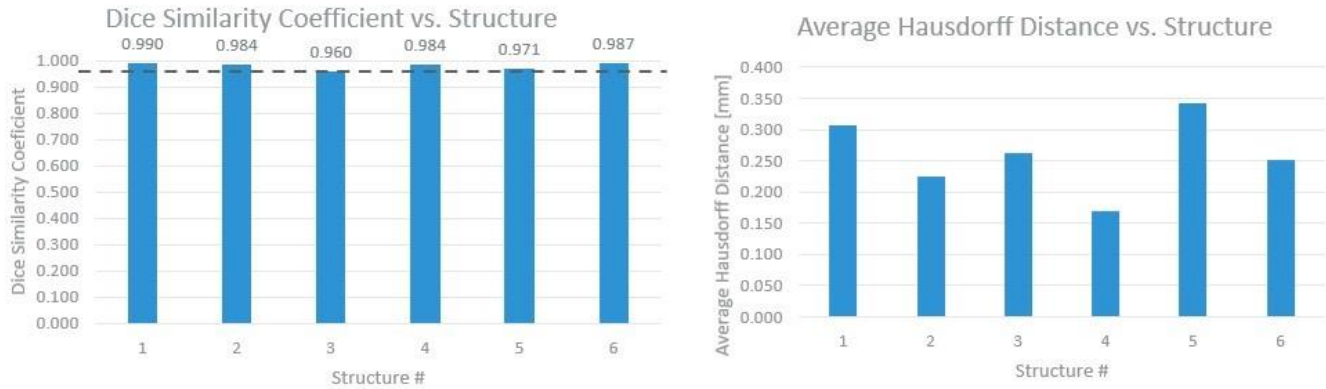


Figure 8: Charts showing the DSC and AHD for each analyzed structure

Results from Retrospective Analysis of Treatment Plans

As mentioned previously, a qualitative analysis of the alignment between the EAM and the patient's CT image was performed for two patients treated at OHSU. It was determined that the unhealthy tissue did not align with the target volumes in both cases (N=2). A cross section of one image registration attempt can be seen below in figure 9.



Figure 9: Cross section of attempted image fusion between one patient's CT image and EAM

Additionally, it was observed that the EAMs were challenging to align with the patient CT images. This mismatch was seen in both cases. This suggests that the fusion of these images is not adequate for at its current state and is not accurate enough to use in radiation therapy applications.

Discussion

In the previous chapters, the details of how XDEM maps XML EAMs to DICOM EAMs were explained, and the results from assessing XDEM were displayed, but not explained. Therefore, this chapter will aim to explain what these results signify, and what this means for the future clinical use of XDEM will be thoroughly discussed.

EnSite™ and 3D Slicer™ Distance Measurement

For this project, the accuracy analysis of XDEM was performed in 3D Slicer™. This was because 3D Slicer™ has the capability to import all relevant medical images involved in this subproject as well as the subproject discussed in the next section. Because 3D Slicer™ has not been assessed by the radiation medicine department at OHSU, it was necessary to prove its accuracy in displaying EAMs before trusting any measures that it calculated, and its ability to display XML EAMs as well as DICOM EAMs.

As seen in table 1, similar distance measurements were conducted in both the EnSite™ Precision software and 3D Slicer™. Once these measurements were obtained, a statistical analysis was performed using a paired 2-tailed t-test. The p-score is shown to be greater than the selected significance level, meaning that these sets of measurements are not statistically different from one another.

XML EAM and DICOM EAM Segment Comparison

For this subproject, the XML EAM and DICOM EAM were compared to validate XDEM's format mapping accuracy. As mentioned above, this was performed by segmenting the

structures in similar XML and DICOM EAMs, registering them, and computing similarity coefficients such as the DSC, HD, and AHD. These steps were all performed within 3D Slicer™.

As mentioned above, the DSC for all structures analyzed were above 0.95, much higher than the tolerance set by TG-132²² which is ~0.8-0.9. This shows that XDEM is accurately reproducing these EAMs in a DICOM format within an acceptable tolerance.

The mean AVD for the structures analyzed was 0.260 mm with a standard deviation of 0.056 mm. These values are far below the PTV margin of 3 mm that is created for the target volumes during ablative cardiac SBRT interventions, giving even more confidence in XDEM's ability to recreate EAMs in a DICOM format from XML data formats.

Retrospective Analysis of Treatment Plans

As shown in the results section, the EAMs were not able to be fused to the patient CT images in an accurate manner. This highlights the challenges associated with fusing these maps to the CT images for use in ablative cardiac SBRT. The mismatch may be due to several factors. One of them could be due to a lack of anatomical landmarks highlighted within the anatomy that was mapped, or that the anatomical landmarks within the anatomy that was mapped were not highlighted. In the future, it may be helpful to highlight landmarks such as valves within the heart, or include anatomy such as the aortic arch, if time permits during the EA mapping procedure. Another factor that could lead to challenges during fusion could be that the heart in both images is displayed at different phases. The CT used for planning is an untagged CT image, and EAMs typically show cardiac tissue during diastole. These factors could be what are leading to the registration inaccuracies, potentially compromising this step of this project. As more of

these procedures are performed and more data is collected, stronger conclusions will be able to be drawn regarding this image registration.

It is also important to note that since the image fusion was unsuccessful, the accuracy of unhealthy tissue displayed on the EAM was difficult to verify. As more data is collected in the future, and image fusion is determined to be accurate, this function of XDEM will be able to be evaluated with more certainty.

Conclusion

In conclusion, this project aimed to create a software tool that would improve treatment planning accuracy, target validation, and clinical efficiency. This was done by validating 3D Slicer's™ ability to display images, confirming that XDEM was mapping XML EAMs to DICOM EAMs with high spatial accuracy, and finally by performing a retrospective analysis on past patient treatment plans to analyze the accuracy of the delineated PTVs. The results showed that the measurements made in 3D Slicer™ were not statistically different than those made in EnSite™. They also showed that XDEM was able to map XML EAMs to DICOM EAMs with high fidelity. Finally, the retrospective analysis showed that it was difficult to confidently fuse patient CTs with EAMs, indicating that further improvements must be made to use XDEM clinically in the future.

Overall, the findings of this project have important implications for the accuracy, precision, and efficiency of radiation therapy treatment planning for ablative cardiac SBRT. The ability of XDEM to accurately map XML EAMs to DICOM EAMs suggests that it could effectively aid treatment planning in the future. However, the ability to accurately fuse these images is a problem that needs to be addressed, which may require the collection of more XML EAM data that includes more anatomical landmarks, or more obvious ones. This may also require collaboration between medical physics and cardiac electrophysiology to better align patient CT images and EAMs. Other future work may include exporting these EAMs in different DICOM forms, such as radiation therapy structure sets or as a PET image so that the image can be displayed in color, similarly to an original EAM.

In summary, this study provides insight into the accuracy and limitations of fusing EAMs to patient CT images for ablative cardiac SBRT and suggests improvements that could be made in the future that would make it possible for XDEM to improve the accuracy, precision, and efficiency of ablative cardiac SBRT, ultimately leading to better patient outcome and lower monetary cost to the clinic.

References

1. Loo BW, Soltys SG, Wang L, et al. Stereotactic Ablative Radiotherapy for the Treatment of Refractory Cardiac Ventricular Arrhythmia. *Circ Arrhythm Electrophysiol.* 2015;8(3):748-750. doi:10.1161/CIRCEP.115.002765
2. Cuculich PS, Schill MR, Kashani R, et al. Noninvasive Cardiac Radiation for Ablation of Ventricular Tachycardia. *N Engl J Med.* 2017;377(24):2325-2336. doi:10.1056/NEJMoa1613773
3. Ventricular tachycardia - Symptoms and causes. Mayo Clinic. Accessed May 14, 2023. <https://www.mayoclinic.org/diseases-conditions/ventricular-tachycardia/symptoms-causes/syc-20355138>
4. Foth C, Gangwani M, Ahmed I, Avley H. *Ventricular Tachycardia*. NIH; 2023. <https://www.ncbi.nlm.nih.gov/books/NBK532954/>
5. Zipes DP, Camm AJ, Borggrefe M, et al. ACC/AHA/ESC 2006 guidelines for management of patients with ventricular arrhythmias and the prevention of sudden cardiac death: A report of the American College of Cardiology/American Heart Association Task Force and the European Society of Cardiology Committee for Practice Guidelines (Writing Committee to Develop Guidelines for Management of Patients With Ventricular Arrhythmias and the Prevention of Sudden Cardiac Death) Developed in collaboration with the European Heart Rhythm Association and the Heart Rhythm Society. *Europace.* 2006;8(9):746-837. doi:10.1093/europace/eul108
6. Antiarrhythmic Drugs: Types, Uses and Side Effects. Cleveland Clinic. Accessed May 10, 2023. <https://my.clevelandclinic.org/health/drugs/22867-what-are-antiarrhythmics>
7. Implantable Cardioverter Defibrillator (ICD). www.heart.org. Accessed May 14, 2023. <https://www.heart.org/en/health-topics/arrhythmia/prevention--treatment-of-arrhythmia/implantable-cardioverter-defibrillator-icd>
8. Santangeli P, Marchlinski FE. Techniques for the provocation, localization, and ablation of non-pulmonary vein triggers for atrial fibrillation. *Heart Rhythm.* 2017;14(7):1087-1096. doi:10.1016/j.hrthm.2017.02.030
9. Wei C, Qian PC, Boeck M, et al. Cardiac stereotactic body radiation therapy for ventricular tachycardia: Current experience and technical gaps. *J Cardiovasc Electrophysiol.* 2021;32(11):2901-2914. doi:10.1111/jce.15259
10. Blanck O, Buergy D, Vens M, et al. Radiosurgery for ventricular tachycardia: preclinical and clinical evidence and study design for a German multi-center multi-platform feasibility trial (RAVENTA). *Clin Res Cardiol.* 2020;109(11):1319-1332. doi:10.1007/s00392-020-01650-9

11. Fiorentino A, Di Monaco A, Surgo A, et al. Linac-based STereotactic Arrhythmia Radioablation (STAR) of ventricular tachycardia: Case report and literature review. *Clin Case Rep*. 2021;9(1):362-366. doi:10.1002/ccr3.3530
12. Knutson NC, Samson PP, Hugo GD, et al. Radiation Therapy Workflow and Dosimetric Analysis from a Phase 1/2 Trial of Noninvasive Cardiac Radioablation for Ventricular Tachycardia. *Int J Radiat Oncol*. 2019;104(5):1114-1123. doi:10.1016/j.ijrobp.2019.04.005
13. Stern RL, Heaton R, Fraser MW, et al. Verification of monitor unit calculations for non-IMRT clinical radiotherapy: Report of AAPM Task Group 114. *Med Phys*. 2011;38(1):504-530. doi:10.1118/1.3521473
14. Low DA, Harms WB, Mutic S, Purdy JA. A technique for the quantitative evaluation of dose distributions. *Med Phys*. 1998;25(5):656-661. doi:10.1118/1.598248
15. How the EnSite Precision Cardiac Mapping System Works. Accessed May 10, 2023. <https://www.cardiovascular.abbott/int/en/hcp/products/electrophysiology/mapping-systems/ensite/about/how-it-works.html>
16. ep-ensite-accuracy-whitepaper.pdf. Accessed May 10, 2023. <https://www.cardiovascular.abbott/content/dam/bss/divisionalsites/cv/hcp/products/electrophysiology/ensite/documents/ep-ensite-accuracy-whitepaper.pdf>
17. Rooney A. *Foundations of Java for ABAP Programmers: Introduces the Core J2SE 5 and Java EE 5 Platform Essentials to the SAP Programmer*. Apress; 2006.
18. Geography Markup Language. Open Geospatial Consortium. Accessed May 10, 2023. <https://www.ogc.org/standard/gml/>
19. Pianykh OS. *Digital Imaging and Communications in Medicine (DICOM)*. Springer Berlin Heidelberg; 2012. doi:10.1007/978-3-642-10850-1
20. McDermott PN, Orton CG. *The Physics & Technology of Radiation Therapy, 2nd Edition*. 2nd edition. Medical Physics Pub Corp; 2018.
21. Saw CB, Chen H, Beatty RE, Wagner H. Multimodality Image Fusion and Planning and Dose Delivery for Radiation Therapy. *Med Dosim*. 2008;33(2):149-155. doi:10.1016/j.meddos.2008.03.001
22. Latifi K, Caudell J, Zhang G, Hunt D, Moros EG, Feygelman V. Practical quantification of image registration accuracy following the AAPM TG-132 report framework. *J Appl Clin Med Phys*. 2018;19(4):125-133. doi:10.1002/acm2.12348
23. Hausdorff distance. Accessed May 10, 2023. <http://cgm.cs.mcgill.ca/~godfried/teaching/cg-projects/98/normand/main.html>
24. Müller D, Soto-Rey I, Kramer F. Towards a guideline for evaluation metrics in medical image segmentation. *BMC Res Notes*. 2022;15(1):210. doi:10.1186/s13104-022-06096-y

25. Kumarasiri A, Siddiqui F, Liu C, et al. Deformable image registration based automatic CT-to-CT contour propagation for head and neck adaptive radiotherapy in the routine clinical setting. *Med Phys*. 2014;41(12):121712. doi:10.1118/1.4901409
26. Fedorov A, Beichel R, Kalpathy-Cramer J, et al. 3D Slicer as an image computing platform for the Quantitative Imaging Network. *Magn Reson Imaging*. 2012;30(9):1323-1341. doi:10.1016/j.mri.2012.05.001
27. What's New In Python 3.9. Python documentation. Accessed May 10, 2023. <https://docs.python.org/3/whatsnew/3.9.html>
28. Welcome to Python.org. Python.org. Published May 5, 2023. Accessed May 10, 2023. <https://www.python.org/>
29. PyCharm: the Python IDE for Professional Developers by JetBrains. JetBrains. Accessed May 10, 2023. <https://www.jetbrains.com/pycharm/>
30. Blanck O, Buergy D, Vens M, et al. Radiosurgery for ventricular tachycardia: preclinical and clinical evidence and study design for a German multi-center multi-platform feasibility trial (RAVENTA). *Clin Res Cardiol Off J Ger Card Soc*. 2020;109(11):1319-1332. doi:10.1007/s00392-020-01650-9
31. Knutson NC, Samson PP, Hugo GD, et al. Radiation Therapy Workflow and Dosimetric Analysis from a Phase 1/2 Trial of Noninvasive Cardiac Radioablation for Ventricular Tachycardia. *Int J Radiat Oncol*. 2019;104(5):1114-1123. doi:10.1016/j.ijrobp.2019.04.005
32. Medical Advisory Secretariat. Advanced electrophysiologic mapping systems: an evidence-based analysis. *Ont Health Technol Assess Ser*. 2006;6(8):1-101.
33. Saw CB, Chen H, Beatty RE, Wagner H. Multimodality image fusion and planning and dose delivery for radiation therapy. *Med Dosim Off J Am Assoc Med Dosim*. 2008;33(2):149-155. doi:10.1016/j.meddos.2008.03.001
34. Foth C, Gangwani MK, Ahmed I, Alvey H. Ventricular Tachycardia. In: *StatPearls*. StatPearls Publishing; 2023. Accessed June 5, 2023. <http://www.ncbi.nlm.nih.gov/books/NBK532954/>